

PAPER • OPEN ACCESS

Antibacterial Performance of Fe₃O₄/PEG-4000 Prepared by Co-precipitation Route

To cite this article: Deny Arista *et al* 2019 *IOP Conf. Ser.: Mater. Sci. Eng.* **515** 012085

View the [article online](#) for updates and enhancements.

Antibacterial Performance of Fe₃O₄/PEG-4000 Prepared by Co-precipitation Route

Deny Arista, Aulia Rachmawati, Nurlailul Ramadhani, Rosy Eko Saputro, Ahmad Taufiq*, Sunaryono

Department of Physics, Faculty of Mathematics and Natural Sciences, Universitas Negeri Malang, Jl. Semarang 5, Malang 65145, Indonesia

*Corresponding author's email: ahmad.taufiq.fmipa@um.ac.id

Abstract: In this paper, we report the synthesis of Fe₃O₄ nanoparticles modifying polyethylene glycol/PEG-4000 by co-precipitation route. The structural and antibacterial features of the samples were studied by means of XRD, SEM, FTIR, and antibacterial test. The results of XRD data showed that Fe₃O₄/PEG was in a spinel cubic structure. The sample presented the combined composition of the Fe₃O₄/PEG-4000 in the nanometric scale in agglomerated form. Interestingly, the Fe₃O₄/PEG-4000 exhibited an excellent performance as an antibacterial agent with the average inhibitory diameter for each *Escherichia Coli* and *Staphylococcus Aureus* bacteria are 1.67 mm and 1.97 mm respectively.

Keywords: Fe₃O₄, PEG-4000, co-precipitation route, iron sand, antibacterial agent.

1. Introduction

Nowadays, nanomaterial evokes interests to be studied due to its broad technology applications, particularly magnetic nanoparticles. From various magnetic nanoparticles, magnetite (Fe₃O₄) receives exceptional attention for various biomedical applications, such as drug delivery [1], hyperthermia [2], and magnetic resonance imaging [3] and antifungal material [4]. Besides that, Fe₃O₄ also has high and non-toxic biocompatibility [5], so it is believed to allow access to a promising medical application as an antimicrobial material especially anti-bacterial [6,7]. The previous study has explored Fe₃O₄ as an antibacterial agent caused by reactive oxygen [8,9].

Several methods have been performed to synthesize Fe₃O₄ nanoparticles among them is co-precipitation [10], sol-gel [11], hydrothermal [12], sonochemical [13] and electrochemical route [14]. In general, co-precipitation is the simplest and most economical method to produce the Fe₃O₄ nanoparticles [15]. However, Fe₃O₄ nanoparticles have fast aggregation-prone properties [16]. Therefore, layers or surfactants, which are able to prevent aggregation and stabilize the Fe₃O₄ nanoparticles, are needed as coating agents [17].

Previous work showed that the coating of Fe₃O₄ using polyethylene glycol/PEG could enhance the biocompatibility properties, high adsorption, and chemical stability [18,19]. Furthermore, PEG can increase the biotechnology application because it is more efficient, particularly PEG-4000 [20,21]. Therefore, in the present research, it is essential to prepare the Fe₃O₄ nanoparticles as an antibacterial



agent. Accordingly, this research studied the Fe_3O_4 nanoparticles which have been modified with PEG-4000 used as an antibacterial agent.

2. Methods

The materials used in this work were iron sand, HCl, NH_4OH , H_2O , PEG-4000, DMSO, ampicillin, peptone, meat extract, agar, *Escherichia coli* and *Staphylococcus aureus* bacteria. The synthesis was initiated by dissolving iron sand, and HCL stirred using a magnetic stirrer. It is then filtered using filter paper (the sediment was discarded). Therefore, the FeCl_3 and FeCl_2 solutions were formed. The solutions were reacted with PEG-4000 solution and then titrated with NH_4OH using a magnetic stirrer until black sediment was formed. The sediment was washed with H_2O until reaching the neutral pH. Next, the sediment was filtered to obtain the $\text{Fe}_3\text{O}_4/\text{PEG}$ particles. Finally, the filtered sediment was deposited and put in the oven for an hour. An antibacterial testing was performed using a well diffusion method. The first step was making the Fe_3O_4 test solution dissolved with DMSO. Next, the creation of medium was done utilizing peptone, meat extract, and agar then proceeded with the bacterial hatchery. Then, making well pits and applying bacteria that have been inoculated to the medium surface. After the pit was formed, the test sample was dripped into the well pits. The last stage was observing the sample's zone of inhibition on *Escherichia coli* and *Staphylococcus aureus* bacteria.

3. Results and Discussion

From Figure 1, it can be seen the results of the X-ray diffraction from $\text{Fe}_3\text{O}_4/\text{PEG}$ nanoparticles. In relation to the phase formation, Rietica software was utilized to identify the success of this synthesis, and the results were plotted according to Figure 1. Based on above diffraction pattern, a peak appears characterizing Fe_3O_4 namely at $2\theta = 30.3^\circ$, 35.4° , 43.3° , 53.7° , 57.3° , 62.9° , and 74.3° which are compatible with (*hkl*) plane of (022), (113), (004), (224), (115), (044), and (533) where the highest peak was at the angle of (2θ) 35.4° on (*hkl*) plane (113). Through the highest peak, it can be found out the particle size by calculating FWHM (β) value from the peak of the diffraction plane. It is where the average size of the crystal is determined by the expansion of X-ray diffraction peaks using Scherrer formulation according to Equation 1 [22].

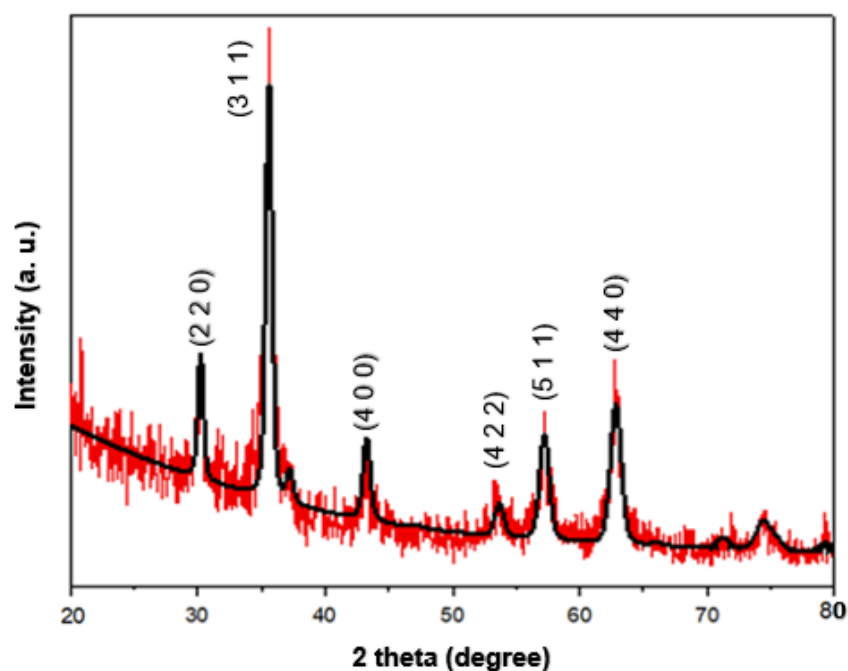


Figure 1. The diffraction pattern of $\text{Fe}_3\text{O}_4/\text{PEG}$ -4000 nanoparticles and its refinement result

$$D = \frac{k\lambda}{\beta \cos \theta} \quad (1)$$

where $k =$ Scherrer constant (0.9)
 $\lambda =$ Wavelength (nm)

$\beta =$ FWHM (radian)
 $\theta =$ Bragg angle (radian)

Based on the analysis of the Fe_3O_4 highest peak expansion, it was obtained the highest peak expansion was at the angle of $(2\theta) 35.44^\circ$, and the FWHM value was 1.88 rad. Thus, according to Equation 1, the crystal size obtained was 13 nm. This value is not significantly different from the crystal size from the refinement result. On the previous report, Kanagasubbulakshmi *et al.* conducted a Fe_3O_4 synthesis with the assistance of natural materials with a sol-gel method and obtaining a bigger particle size, namely in the range between 14 nm to 18 nm [23]. Another report, Chen *et al.* performed Fe_3O_4 particle synthesis using a hydrothermal method and obtaining a diameter of 30 nm [24]. Therefore, the coprecipitation method is proven effective in synthesizing the magnetic nanoparticle with a relatively small size. The shape of the crystal structure of Fe_3O_4 was inverse spinel cubic which can be observed using the diamond software as seen in Figure 2.

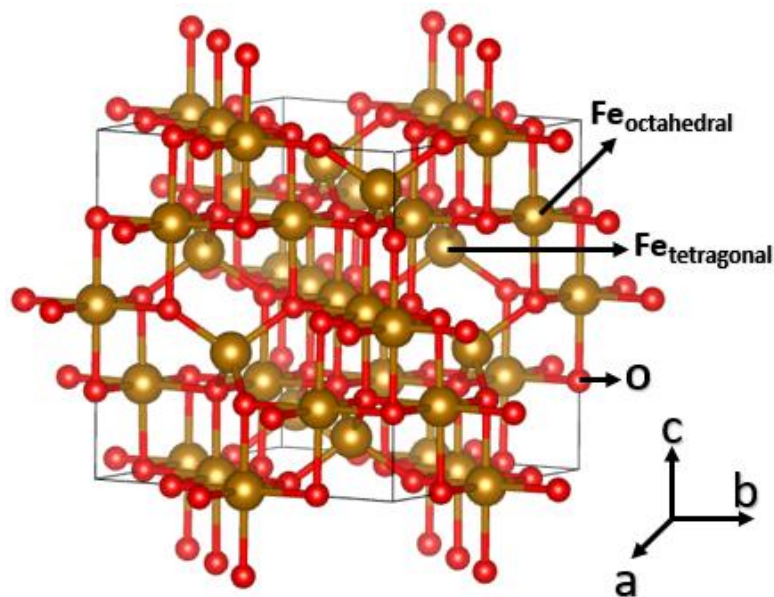


Figure 2. The Fe_3O_4 crystal structure

Based on Figure 2, the green-colored atom represents Fe atom forming the tetragonal site, the blue-colored atom represents Fe atom forming the octahedral site, and the red-colored atom represents O atom. All Fe^{2+} ions occupied half of the octahedral site and Fe^{3+} is shared equally to the rest of octahedral and tetrahedral sites [25]. The crystal structure of Fe_3O_4 is inverse-spinel cubic [26] which shows the structural differences with other Fe derivative compounds such as maghemite (cubic with a space group of $P4_132$) [27] and hematite (rhombohedral) [28]. This is also affected by reaction stages of Fe_3O_4 formation as seen in Equation 2-4 [29]:



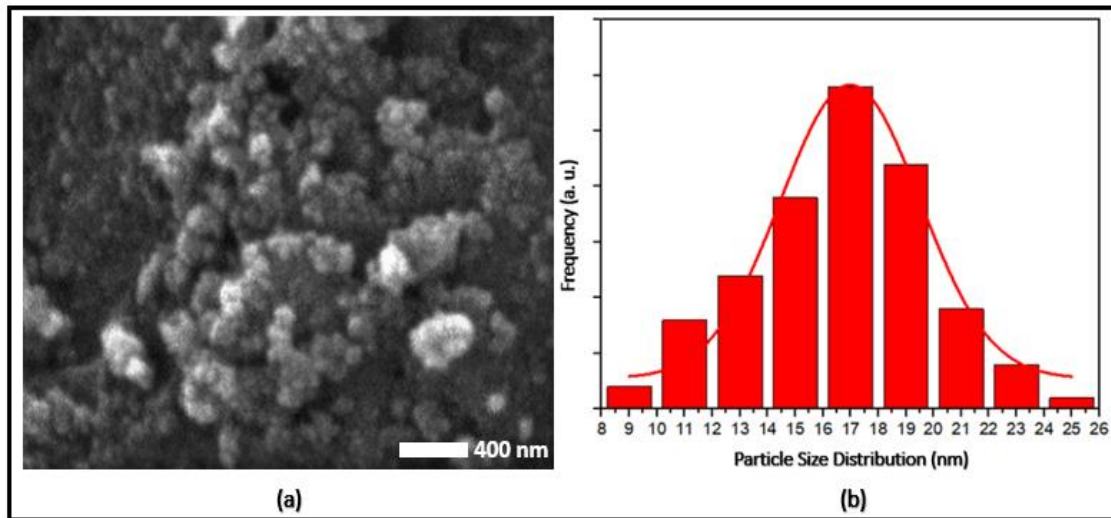


Figure 3. (a) The morphology and (b) size distribution of Fe_3O_4

Figure 3 shows that the uniformity of $\text{Fe}_3\text{O}_4/\text{PEG}$ nanoparticles and Fe_3O_4 nanoparticles has been achieved. This nanoparticle has the average size of 17 nm. Nanoparticle consists of fine particles with regular ball morphology with a little agglomeration. The agglomeration phenomenon is a natural tendency owned by Fe_3O_4 nanoparticle due to the Van der Waals force and also the pulse of a magnetic dipole. Therefore, the nanoparticles form the distributed cluster with the most dominant size which is around 17 nm. Visually, it can be seen that there is a white-colored particle which represents PEG 4000 used in Fe_3O_4 synthesis. This shows that Fe_3O_4 nanoparticle is well bound with PEG 4000 and becomes a proof that the coprecipitation method is efficient in the synthesis of $\text{Fe}_3\text{O}_4/\text{PEG}$ 4000 nanoparticle.

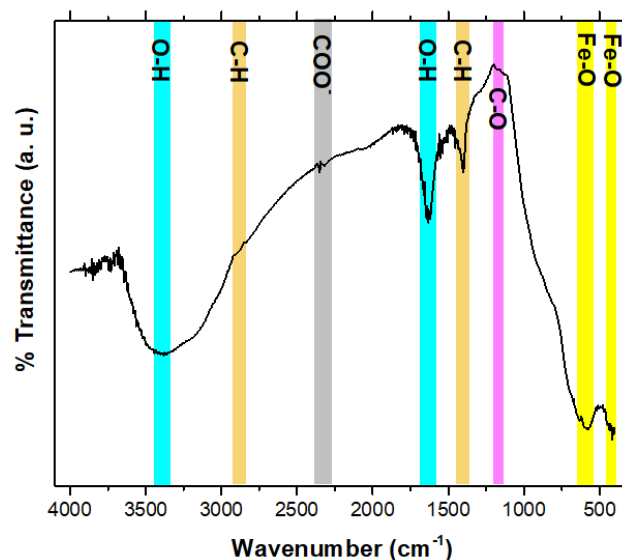


Figure 4. The Functional groups of $\text{Fe}_3\text{O}_4/\text{PEG}$

Figure 4 shows the FT-IR spectrum from $\text{Fe}_3\text{O}_4/\text{PEG}$. The main functional group which characterized the existence of Fe_3O_4 located in the area of 416.4 cm^{-1} represents Fe atom in tetragonal site and in the area of 568.4 cm^{-1} for Fe atom on octahedral site spinel structure [30]. The peak on the area of 1613.7 cm^{-1} and 3400.5 cm^{-1} shows there is an OH bond accompanying the formation reactions using a

coprecipitation method [31]. Furthermore, there are several peaks characterizing the functional group of PEG-4000, namely in the area of 1174.6 cm^{-1} which is a C-O bond, the peak on the area of 1402.2 cm^{-1} and 2887.1 cm^{-1} which represents the existence of COO^- bound [32–34]. Through the characterization using the above FTIR, it can be claimed that between Fe_3O_4 and PEG-4000 have a bound both through a synthesis process of coprecipitation.

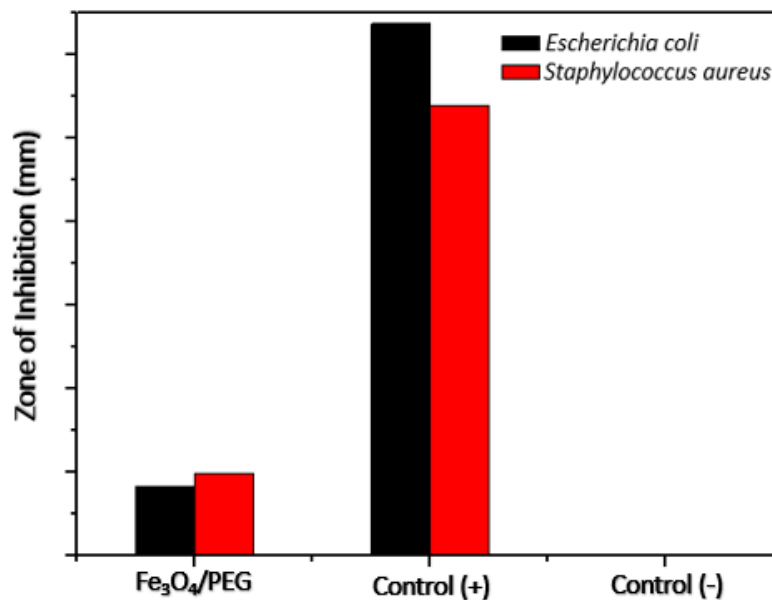


Figure 5. The antibacterial activity on *E. coli* and *S. aureus* bacteria

The antibacterial testing used a well diffusion method and the bacteria used were *Escherichia coli* and *Staphylococcus aureus*. The well diffusion method showed the diameter of the antibacterial inhibitory zone. The antibacterial testing results shown in Figure 5 indicate that $\text{Fe}_3\text{O}_4/\text{PEG}$ -4000 has the inhibitory power on *Escherichia coli* and *Staphylococcus aureus* bacteria. From the testing result, it also shows that $\text{Fe}_3\text{O}_4/\text{PEG}$ -4000 has potentials in inhibiting *Escherichia coli* and *Staphylococcus aureus* bacteria. In the previous research, Sheikh *et al* show the antibacterial results for ferrofluid samples with Fe_3O_4 filler, with the same rate of Fe_3O_4 as in this research, the results that they obtained is approximately 1.7 mm [35]. In this study, Fe_3O_4 which was modified by PEG-4000 has the inhibitory power of 1.67 and 1.97 for *Escherichia coli* and *Staphylococcus aureus* bacteria respectively. However, the increased performance of Fe_3O_4 is still relatively low since it only relies on the ability of reactive oxygen species which is contained inside it [36]. Therefore, for the future research, a performance improvement of Fe_3O_4 nanoparticle needs to be conducted from the aspect of structural modification both with the doping [37] and nanocomposite techniques [38].

4. Conclusion

The size of Fe_3O_4 nanoparticle modified by PEG-4000 was 12.21 nm. Fe_3O_4 nanoparticles with a spherical shape experienced an agglomeration with the size of 17 nm. $\text{Fe}_3\text{O}_4/\text{PEG}$ -4000 has potentials in inhibiting *Escherichia coli* and *Staphylococcus aureus* bacteria. However, $\text{Fe}_3\text{O}_4/\text{PEG}$ -4000 is more effective in inhibiting the growth of *Staphylococcus aureus* bacteria. The average numbers of inhibitory power are 1.67 nm and 1.97 nm respectively.

References

- [1] Dutta B, Shetake N G, Barick B K, Barick K C, Pandey B N, Priyadarsini K I and Hassan P A 2018 Ph sensitive surfactant-stabilized Fe₃O₄ magnetic nanocarriers for dual drug delivery *Colloids and Surfaces B: Biointerfaces* **162** 163–71
- [2] Arriortua O K, Insausti M, Lezama L, de Muro I G, Garaio E, de la Fuente J M, Fratila R M, Morales M P, Costa R and Eceiza M 2018 RGD-Functionalized Fe₃O₄ nanoparticles for magnetic hyperthermia *Colloids and Surfaces B: Biointerfaces* **165** 315–24
- [3] Wang T, Hou Y, Bu B, Wang W, Ma T, Liu C, Lin L, Ma L, Lou X and Gao M 2018 MRI Probes: Timely Visualization of the Collaterals Formed during Acute Ischemic Stroke with Fe₃O₄ Nanoparticle-based MR Imaging Probe (Small 23/2018) *Small* **14** 1870108
- [4] Seddighi N S, Salari S and Izadi A R 2017 Evaluation of antifungal effect of iron-oxide nanoparticles against different Candida species *IET Nanobiotechnology* **11** 883–8
- [5] Habibi N 2014 Preparation of biocompatible magnetite-carboxymethyl cellulose nanocomposite: characterization of nanocomposite by FTIR, XRD, FESEM and TEM *Spectrochimica Acta Part A: Molecular and Biomolecular Spectroscopy* **131** 55–8
- [6] Venkateswarlu S, Kumar B N, Prathima B, Anitha K and Jyothi N V V 2015 A novel green synthesis of Fe₃O₄-Ag core shell recyclable nanoparticles using Vitis vinifera stem extract and its enhanced antibacterial performance *Physica B: Condensed Matter* **457** 30–5
- [7] Rădulescu M, Andronescu E, Holban A M, Vasile B S, Iordache F, Mogoantă L, Mogoșanu G D, Grumezescu A M, Georgescu M and Chifiriuc M C 2016 Antimicrobial Nanostructured Bioactive Coating Based on Fe₃O₄ and Patchouli Oil for Wound Dressing *Metals* **6** 103
- [8] Wang X, Cai A, Wen X, Jing D, Qi H and Yuan H 2017 Graphene oxide- Fe₃O₄ nanocomposites as high-performance antifungal agents against Plasmopara viticola *Science China Materials* **60** 258–68
- [9] Nazari A, Shishehbor M R and Poorhashemi S M 2016 Enhanced magnetic and antifungal characteristics on wool with Fe₃O₄ nanoparticles and BTCA: a facile synthesis and RSM optimization *The Journal of The Textile Institute* **107** 1617–31
- [10] Arévalo P, Isasi J, Caballero A C, Marco J F and Martín-Hernández F 2017 Magnetic and structural studies of Fe₃O₄ nanoparticles synthesized via coprecipitation and dispersed in different surfactants *Ceramics International* **43** 10333–40
- [11] Li J, Wu Y, Yang M, Yuan Y, Yin W, Peng Q, Li Y and He X 2017 Electrospun Fe₂O₃ nanotubes and Fe₃O₄ nanofibers by citric acid sol-gel method *Journal of the American Ceramic Society* **100** 5460–70
- [12] Hedayati K, Goodarzi M and Ghanbari D 2017 Hydrothermal synthesis of Fe₃O₄ nanoparticles and flame resistance magnetic poly styrene nanocomposite *Journal of Nanostructures* **7** 32–9
- [13] Badnore A U, Salvi M A, Jadhav N L, Pandit A B and Pinjari D V 2018 Comparison and characterization of Fe₃O₄ nanoparticles synthesized by conventional magnetic stirring and sonochemical method *Advanced Science Letters* **24** 5681–6
- [14] Karimzadeh I, Aghazadeh M, Doroudi T, Reza Ganjali M and Hossein Kolivand P 2017 Effective Preparation, Characterization and In Situ Surface Coating of Superparamagnetic Fe₃O₄ Nanoparticles with Polyethyleneimine Through Cathodic Electrochemical Deposition (CED) *Current Nanoscience* **13** 167–74
- [15] Bindhu M R, Rakhi R B, Umadevi M and Anjana P M 2018 Antimicrobial, electrochemical and photo catalytic activities of Zn doped Fe₃O₄ nanoparticles
- [16] Wang H, Zhao X, Han X, Tang Z, Liu S, Guo W, Deng C, Guo Q, Wang H and Wu F 2017 Effects of monovalent and divalent metal cations on the aggregation and suspension of Fe₃O₄ magnetic nanoparticles in aqueous solution *Science of the Total Environment* **586** 817–26
- [17] Celis J A, Mejía O O, Cabral-Prieto A, García-Sosa I, Derat-Escudero R, Saitovitch E B and Camarena M A 2017 Synthesis and characterization of nanometric magnetite coated by oleic acid and the surfactant CTAB *Hyperfine Interactions* **238** 43
- [18] Kurniawan C, Eko A S, Ayu Y S, Sihite P T A, Ginting M, Simamora P and Sebayang P 2017

- Synthesis and Characterization of Magnetic Elastomer based PEG-Coated Fe₃O₄ from Natural Iron Sand *IOP Conference Series: Materials Science and Engineering* vol 202 (IOP Publishing) p 012051
- [19] Anbarasu M, Anandan M, Chinnasamy E, Gopinath V and Balamurugan K 2015 Synthesis and characterization of polyethylene glycol (PEG) coated Fe₃O₄ nanoparticles by chemical co-precipitation method for biomedical applications *Spectrochimica Acta Part A: Molecular and Biomolecular Spectroscopy* **135** 536–9
- [20] Eatemadi A, Darabi M, Afraidooni L, Zarghami N, Daraee H, Eskandari L, Mellatyar H and Akbarzadeh A 2016 Comparison, synthesis and evaluation of anticancer drug-loaded polymeric nanoparticles on breast cancer cell lines *Artificial cells, nanomedicine, and biotechnology* **44** 1008–17
- [21] Guizani M, Maeda T, Ito R and Funamizu N 2018 Synthesis and Characterization of Magnetic Nanoparticles as a Candidate Draw Solution for Forward Osmosis *Journal of Water and Environment Technology* **16** 63–71
- [22] Shete P B, Patil R M, Tiwale B M and Pawar S H 2015 Water dispersible oleic acid-coated Fe₃O₄ nanoparticles for biomedical applications *Journal of Magnetism and Magnetic Materials* **377** 406–10
- [23] Kanagasubbulakshmi S and Kadirvelu K 2017 Green Synthesis of Iron Oxide Nanoparticles using *Lagenaria Siceraria* and Evaluation of its Antimicrobial Activity *Defence Life Science Journal* **2** 422–7
- [24] Chen Z, Du Y, Li Z, Yang K and Lv X 2017 Controllable synthesis of magnetic Fe₃O₄ particles with different morphology by one-step hydrothermal route *Journal of Magnetism and Magnetic Materials* **426** 121–5
- [25] Wu W, Wu Z, Yu T, Jiang C and Kim W-S 2015 Recent progress on magnetic iron oxide nanoparticles: synthesis, surface functional strategies and biomedical applications *Science and technology of advanced materials* **16** 023501
- [26] Taimoory S M, Trant J F, Rahdar A, Aliahmad M, Sadeghfar F and Hashemzaei M 2017 Importance of the inter-electrode distance for the electrochemical synthesis of magnetite nanoparticles: Synthesis, characterization, computational modelling, and cytotoxicity *e-Journal of Surface Science and Nanotechnology* **15** 31–9
- [27] Fock J, Bogart L K, González-Alonso D, Espeso J I, Hansen M F, Varón M, Frandsen C and Pankhurst Q A 2017 On the ‘centre of gravity’ method for measuring the composition of magnetite/maghemite mixtures, or the stoichiometry of magnetite-maghemite solid solutions, via 57Fe Mössbauer spectroscopy *Journal of Physics D: Applied Physics* **50** 265005
- [28] Sanson A, Mathon O and Pascarelli S 2014 Local vibrational dynamics of hematite (α -Fe₂O₃) studied by extended x-ray absorption fine structure and molecular dynamics *The Journal of chemical physics* **140** 224504
- [29] Fu S, Wang S, Zhang X, Qi A, Liu Z, Yu X, Chen C and Li L 2017 Structural effect of Fe₃O₄ nanoparticles on peroxidase-like activity for cancer therapy *Colloids and Surfaces B: Biointerfaces* **154** 239–45
- [30] Abboud M, Youssef S, Podlecki J, Habchi R, Germanos G and Foucaran A 2015 Superparamagnetic Fe₃O₄ nanoparticles, synthesis and surface modification *Materials Science in Semiconductor Processing* **39** 641–8
- [31] Ma J, Chang J, Ma H, Zhang D, Ma Q and Wang S 2017 Lengthy one-dimensional magnetite (Fe₃O₄) sub-microfibers with excellent electrochemical performance *Journal of colloid and interface science* **498** 282–91
- [32] Ayashi N, Fallah-Mehrjardi M and Kiasat A R 2017 Synthesis and characterization of a novel nanomagnetic phase-transfer catalyst and its application to regioselective synthesis of β -azido and β -nitro alcohols in water *Russian Journal of Organic Chemistry* **53** 846–52
- [33] Veisi H, Nikseresht A, Rostami A and Hemmati S 2018 Fe₃O₄@ PEG core/shell nanoparticles as magnetic nanocatalyst for acetylation of amines and alcohols using ultrasound irradiations

- under solvent-free conditions *Research on Chemical Intermediates* 1–14
- [34] Chang M, Chang Y-J, Chao P Y and Yu Q 2018 Exosome purification based on PEG-coated Fe₃O₄ nanoparticles *PloS one* **13** e0199438
- [35] Sheikh L, Vohra R, Verma A K and Nayar S 2015 Biomimetically Synthesized Aqueous Ferrofluids Having Antibacterial and Anticancer Properties *Materials Sciences and Applications* **6** 242
- [36] Ma S, Zhan S, Jia Y and Zhou Q 2015 Superior antibacterial activity of Fe₃O₄-TiO₂ nanosheets under solar light *ACS applied materials & interfaces* **7** 21875–83
- [37] Muthukumar H, Mohammed S N, Chandrasekaran N, Sekar A D, Pugazhendhi A and Matheswaran M 2018 Effect of iron doped Zinc oxide nanoparticles coating in the anode on current generation in microbial electrochemical cells *International Journal of Hydrogen Energy*
- [38] Padhi D K, Panigrahi T K, Parida K, Singh S K and Mishra P M 2017 Green synthesis of Fe₃O₄/RGO nanocomposite with enhanced photocatalytic performance for Cr (VI) reduction, phenol degradation, and antibacterial activity *ACS Sustainable Chemistry & Engineering* **5** 10551–62

Acknowledgements

This work is supported by PNB research grant UM 2018.